



Observation of Free-Electron-Laser-Induced Collective Spontaneous Emission (Superfluorescence)

Mitsuru Nagasono,^{1,*} James R. Harries,^{2,1} Hiroshi Iwayama,^{3,4,1} Tadashi Togashi,⁵ Kensuke Tono,⁵ Makina Yabashi,^{1,5} Yasunori Senba,⁵ Haruhiko Ohashi,^{1,5} Tetsuya Ishikawa,¹ and Eiji Shigemasa^{3,4,1}

¹RIKEN/SPring-8, Kouto 1-1-1, Sayo, Hyogo, 679-5148 Japan

²JAEA/SPring-8, Kouto 1-1-1, Sayo, Hyogo, 679-5148 Japan

³UVSOR, IMS, Nishigo-Naka 38, Myodaiji, Okazaki, Aichi 444-8585, Japan

⁴SOKENDAI, Nishigo-Naka 38, Myodaiji, Okazaki, Aichi 444-8585, Japan

⁵JASRI/SPring-8, Kouto 1-1-1, Sayo, Hyogo, 679-5198 Japan

(Received 23 July 2011; published 1 November 2011)

We have observed and characterized 501.6 nm collective spontaneous emission (superfluorescence) following $1s^2 \rightarrow 1s3p$ excitation of helium atoms by 53.7 nm free-electron laser radiation. Emitted pulse energies of up to 100 nJ are observed, corresponding to a photon number conversion efficiency of up to 10%. We observe the peak intensity to scale as ρ^2 and the emitted pulse width and delay to scale as ρ^{-1} , where ρ is the atom number density. Emitted pulses as short as 1 ps are observed, which corresponds to a rate around 75 000 times faster than the spontaneous $1s3p \rightarrow 1s2s$ decay rate. To our knowledge, this is the first observation of superfluorescence following pumping in the extreme ultraviolet wavelength region, and extension of the technique to the generation of extreme ultraviolet and x-ray superfluorescence pulses should be straightforward by using suitable atomic systems and pump wavelengths.

DOI: 10.1103/PhysRevLett.107.193603

PACS numbers: 42.50.Nn, 41.60.Cr, 42.65.Re

Techniques for producing coherent, ultrafast, intense radiation in the UV, extreme ultraviolet (EUV), and x-ray wavelength regions are currently being advanced on three fronts: large-scale free-electron-laser (FEL) user facilities [1–5], high-harmonic generation making use of strong-field ionization [6,7], and also approaches for lasing in atomic media at short wavelengths [8,9]. The combination of techniques also shows potential, for example, by using a free-electron laser as a pump source [10–13] to create gain. This approach is to create an inversion by using the FEL to excite or ionize a gas or foil target, creating an amplified spontaneous emission single-pass laser. Such techniques offer potentially narrower linewidths and shorter, more highly coherent pulses, compared to the seed sources. A hitherto unexplored (but suggested [14]) possibility is making use of the phenomenon of collective spontaneous decay, or superradiance, where an ensemble of excited atoms collectively decay, completely depleting the inversion in a time much shorter than the radiative lifetime of the upper state. Here, we present an experimental observation of superfluorescence (extended-sample superradiance) at 501.6 nm ($1s3p \rightarrow 1s2s$) in helium gas following pumping of the 53.7 nm $1s^2 \rightarrow 1s3p$ transition with 100 fs EUV-FEL pulses from the SPring-8 Compact SASE Source (SCSS) test accelerator [1]. Figure 1 shows the excitation scheme. We observe photon number conversion efficiencies of up to 10%. Superfluorescence is potentially the most efficient approach for extracting the energy stored in an inverted medium. In comparison to the chaotic profiles, “spiky” in both wavelength and temporal distribution,

characteristic of self-amplification by spontaneous emission (SASE) FEL sources, superfluorescence pulses are monochromatic, with a well-defined temporal width. The pulses are emitted with a characteristic delay with respect to the pump pulse, suggesting the possibility of jitter-free, two-color pump-probe experiments, either pairing the superfluorescence pulse with the seed FEL pulse or making use of a cascade of superfluorescent transitions in the same system. In this initial Letter, we demonstrate superfluorescence in the visible region following pumping in the EUV region; however, the technique can be easily

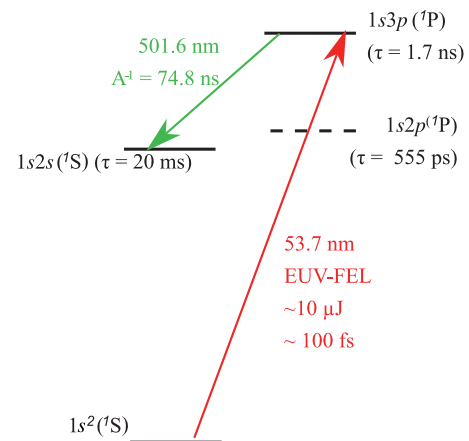


FIG. 1 (color). The excitation scheme. The $1s3p$ state is excited by 53.7 nm wavelength EUV-FEL radiation (red arrow), and superfluorescence is observed at 501.6 nm on the $1s3p \rightarrow 1s2s$ transition (green arrow).

extended to the EUV and x-ray regions by a suitable choice of system and pump wavelength.

Superradiance was first described by Dicke in 1954 [15] for the case where the spatial extent of the inversion in any direction is shorter than the transition wavelength. Over the subsequent 50 years, theoretical and experimental studies have confirmed superradiant (retermed superfluorescent) effects for larger samples, with the looser constraint that the interatom spacing must be less than the wavelength (i.e., a number of excited atoms per cubic wavelength greater than one [16]). Recently, superfluorescence pulses have been observed and characterized from laser-cooled rubidium [17], and pulse lengths on the picosecond time scale observed [18]. “Single-photon” superradiance has also been discussed [19]. Compared to other systems, atomic helium is attractive, since it is readily studied theoretically and offers several possibilities for generating superfluorescence pulses at EUV wavelengths and beyond. In particular, nonautoionizing doubly excited states [20] may be a potential upper state for superfluorescence at ~ 30 nm.

The characteristic feature of superfluorescence is that the ensemble of excited atoms decays collectively. For a cylindrical sample with a Fresnel number F of around 1, the temporal width is given [16] by $\tau_{\text{SF}} = 8\pi/(3\lambda^2\Gamma\rho L)$, where Γ is the natural decay rate of the transition ($1.3 \times 10^7 \text{ s}^{-1}$ for $3p \rightarrow 2s$ in He), λ the wavelength of the transition (501.6 nm), ρ the number density of excited atoms, and L the length of the distribution of excited atoms. There is a delay with respect to the pump pulse, given by $\tau_D = \tau_{\text{SF}}(\ln\sqrt{2\pi N})^2/4$, where $N = \rho V$ is the total number of excited atoms and V is the volume occupied by the excited atoms. Since the temporal width scales as $1/\rho$, the peak intensity of the pulse scales as ρ^2 . For the long thin cylinder geometry ($F \gtrsim L\lambda$), the width is independent of the cross-sectional area but scales as $1/L$. For transversely (instantaneously) excited samples, there is a limit on L , since, if the delay is shorter than the time necessary for light emitted from one end of the sample to reach the other, then the sample must be treated as multiple regions which decay separately [21]. In this case, the delay and width scale as $1/\sqrt{\rho}$. Since we use longitudinal, swept inversion, no such limit on L is expected, although $1/\sqrt{\rho}$ scaling has been observed in swept inversion superfluorescence in Ca vapor [21].

In our study, the length of the sample is limited to $L < 44$ mm by the use of a cubic gas cell. Helium gas is expanded into the cell through a pulsed nozzle, synchronized to the FEL pulses at 30 Hz. The base pressure of the vacuum chamber is less than 1×10^{-6} Pa, rising to a maximum of around 5×10^{-2} Pa with a gas line pressure of 10 atm. From gas flow calculations, we estimate the peak gas pressure in the cell to vary from around 300 to 3000 Pa for pressures behind the pulsed valve of 0.5 to 10 atm. For 300 Pa, the number density of ground-state

helium atoms is around $7 \times 10^{16} \text{ cm}^{-3}$, which corresponds to around 10 000 atoms per cubic 501.6 nm (the wavelength of the superfluorescent transition). Two apertures of diameter 1 mm allow the FEL beam and radiation emitted along the same axis to enter and exit the cell, and additional evacuation occurs through an 18 mm aperture. The FEL radiation is focused at the center of the cell to a full width at half maximum (FWHM) waist radius of around $10 \mu\text{m}$ using a cylindrical and elliptical mirror pair [22]. The M^2 parameter of the beam is 2.9, giving a FWHM beam waist radius at the entrance and exit of the gas cell of around $75 \mu\text{m}$. The peak pulse energy at the exit of the undulator of around $30 \mu\text{J}$ is reduced to around $10 \mu\text{J}$ in the gas cell due to the transmission of the beam line optics. The pulse energy is determined shot-by-shot using a photoion yield detector located upstream of the focusing system and downstream of an argon gas cell which can be used to attenuate the beam. The temporal pulse width is around 100 fs, and, for a pulse energy of $10 \mu\text{J}$, this gives a peak intensity of $3 \times 10^{13} \text{ W} \cdot \text{cm}^{-2}$. From the excitation cross section of the $1s2 \rightarrow 1s3p$ transition [23,24], we can estimate a saturation intensity of around $10^7 \text{ W} \cdot \text{cm}^{-2}$. Taking into account the linewidth of the transition, we estimate the maximum volume in which $3p$ excitation occurs to be of the order of 1 mm^3 .

Visible radiation emitted in the direction of the incident beam was observed through a fused silica viewport in the vacuum chamber containing the gas cell. The 501.6 nm radiation (wavelength confirmed using a fiber-optic spectrometer) observed was highly directional, with a maximum divergence of less than 20 mrad as determined from CCD camera images recorded at two different distances from the center of the gas cell. This divergence was observed to vary shot-by-shot and depend on both FEL intensity and helium gas pressure. The general trend was for lower divergence at higher intensities and pressures, consistent with the predictions for superfluorescence [25]. Rotating a polarizing filter in the beam path showed that the fluorescence was linearly polarized to a high degree, with a horizontal polarization vector. This is the same polarization as the incident FEL radiation, consistent with (but not necessary for) our superfluorescence interpretation. Using a calibrated photodiode, we determined the maximum pulse energy of the emitted radiation to be around 100 nJ, which corresponds to around 2.5×10^{11} photons. For a $5 \mu\text{J}$ FEL pulse (the peak pulse energy observed when the photodiode was being used), this corresponds to a photon number conversion efficiency of around 10%.

To confirm the observation of superfluorescence, we have determined the scaling laws for the observed pulse width and delay by recording the time profile of the emitted 501.6 nm pulses using a Hamamatsu Photonics FESCA 200 streak camera, synchronized to the 30 Hz FEL pulses. Figure 2 shows representative spectra recorded at different

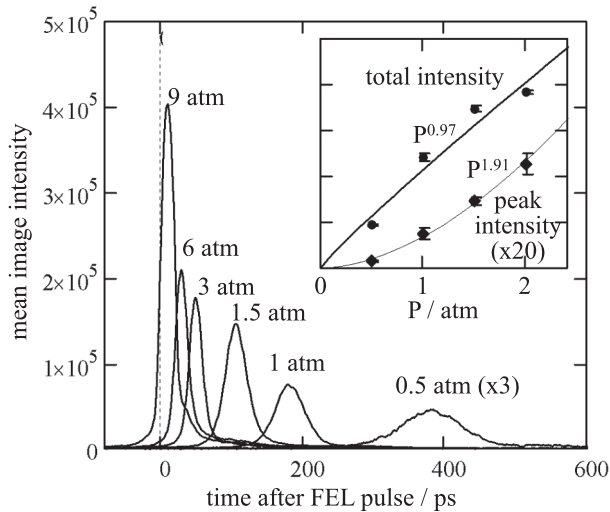


FIG. 2. Representative streak camera data. Each trace is the average of several traces recorded at each gas pressure. The time corresponding to zero delay has been found by fitting—see text and Fig. 3. The inset shows the pressure dependence of the peak and integrated intensity for pressures up to 2 atm (see text), with error bars corresponding to the statistical variance of the data.

gas line pressures. The x axis corresponds to the time delay following the incident FEL pulse, and the y axis to the integrated intensity of the streak camera image. The general trend is that higher gas pressures (i.e., higher ρ) lead to narrower pulses, higher peak intensities, and shorter delay times. To investigate the scaling laws, we extract the peak intensity, integrated intensity, pulse width, and delay for many FEL pulses at each gas line pressure. In an attempt to remove the dependence on the FEL intensity, which varies shot-by-shot, we select five streak camera traces for each gas pressure which correspond to similar FEL pulse energies. For each of these traces, we take the delay as being the position of peak intensity and the width as the full width at half maximum.

Figure 3 shows the mean delay and width observed for each gas line pressure. The delays have been fitted to an equation of the form $\tau = aP^b + c$, where P is the gas line pressure. The offset c accounts for the arbitrary offset of the streak camera trigger with respect to the FEL pulses (which has an inherent jitter of around 30 ps). To account for the resolution of the streak camera, which is a nominal 30 ps FWHM for the 500 ps range used, we have fitted the widths to an equation of the form $\tau^2 = aP^{2b} + c$. The fitted exponents are -1.2 ± 0.1 for the delay and -1.1 ± 0.3 for the width, where the errors have been estimated from the variation of χ^2 . These values are consistent with the $1/\rho$ scaling predicted for pure superfluorescence. Since the width scales as $1/\rho$, it is reasonable to expect that the peak intensity should scale as ρ^2 . However, the increase in peak intensity of the streak camera images was found to level off with increasing gas pressure. We attribute this to the fact that the divergence of the

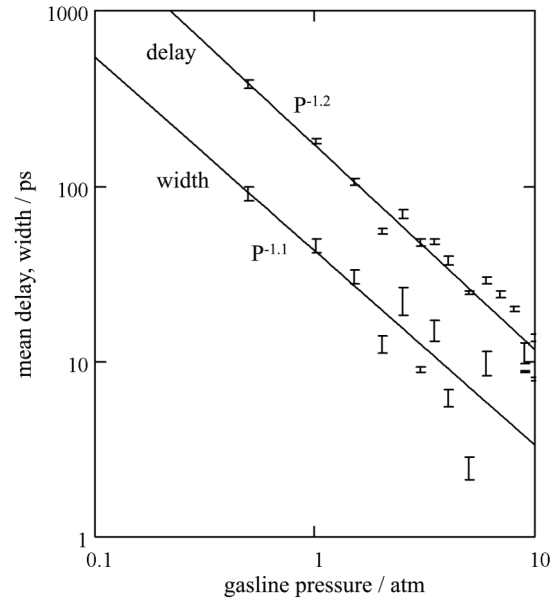


FIG. 3. Pressure dependence of the observed pulse delay and width. The solid lines represent fits to the data of the form $\tau = aP^b + c$ for the delay and $\tau^2 = aP^{2b} + c$ for the width. The offsets c have been subtracted from the data for clarity, and the error bars represent the statistical variance of the extracted values.

superfluorescence beam depends on the emitted intensity. Since the slit at the entrance to the streak camera was narrower than the emitted beam, the transmission also became a function of divergence, and hence gas pressure. Imperfect alignment further complicated the dependence, but, for gas pressures below 2.5 atm, we observe scaling as $\rho^{1.00 \pm 0.05}$ for the total intensity and as $\rho^{1.9 \pm 0.2}$ for the peak intensity, consistent with pure superfluorescence (see the inset to Fig. 2). The effect of pressure-dependent transmission has no effect on the observed delays and temporal widths.

From measurements with a calibrated photodiode, we know that between 10^9 and 10^{11} photons are emitted in each superfluorescence pulse, giving us a direct estimate for N , the number of excited atoms involved in collective emission. Thus, we can calculate $\tau_D/\tau_{SF} = (\ln\sqrt{2\pi N})^2/4$ as being between around 32 and 46. It is clear from Fig. 3 that we observe ratios closer to around 5, which would correspond to a value of N of around 10^3 —inconsistent with the photodiode results. We postulate that the reason for this discrepancy is that we are actually observing superfluorescence from many different regions within the sample, created due to the nonuniform, spiky nature of the pump radiation. A detailed modeling of the shot-by-shot distribution of excited atoms is beyond the scope of this Letter, but we note that the competition between resonant $1s \rightarrow 3p$ excitation, resonant and nonresonant two-photon ionization, and possibly resonant or nonresonant three-photon excitation to doubly excited states or ionization

must be considered [26–28]. In general, the pulse width will vary with the size and shape of each region. The delay will vary only weakly with size but will have an inherent statistical “jitter” which has been predicted to be $2.3/\ln N$ [29], around 10% for $N = 10^9$, of the same order as the $\sim 20\%$ we observe. For a superposition of many individual pulses, we will observe an average delay which represents the experimental conditions, but the observed width will be much broader than the width of each individual superfluorescence pulse, which can be expected to be of the order of a picosecond or less. While the majority of the streak camera traces recorded at each gas pressure show a simple Gaussian-like line shape, we observed occasional traces which appeared to be the superposition of many peaks, consistent with this interpretation. A small number of traces showing “ringing,” where the superfluorescence pulse is partially reabsorbed, leading to a subsequent echo pulse, were also observed.

In summary, we have observed the generation of intense (up to $\sim 10^{11}$ photons per pulse), directional, fast (picosecond-order), linearly polarized radiation at 501.6 nm following $1s^2 \rightarrow 1s3p$ excitation of helium gas using 53.7 nm FEL radiation. Photon number conversion efficiencies of up to 10% are obtained. By studying the scaling with the atom number density of the duration and delay of the output pulses, we attribute the process to superfluorescence on the $1s3p \rightarrow 1s2s$ transition. While we appear to observe the superposition of many superfluorescence pulses from multiple regions, the extent of the inversion and the pulse width and delay of the emitted pulse can be controlled by a judicious choice of experimental setup, and it should be possible to select parameters where superfluorescence from a single region can be generated. Our work represents the first attempt to observe (and exploit) superfluorescence in the EUV region and beyond, with an eye on creating monochromatic x-ray radiation pulses by pumping gaseous, ionic, or solid systems using pulses from one of the new x-ray SASE-FEL sources. This offers a complementary approach to current and proposed schemes for “seeded” FEL sources [30]. We can also conclude that it may be necessary to consider whether the cooperative decay of ensembles of excited atoms has played a part in any of the other FEL-induced nonlinear optical effects reported to date. The nanoparticles and biological molecules which have been the subjects of FEL-based coherent diffraction imaging experiments [31,32] also contain large numbers of atoms of the same element, which may undergo cooperative decay following excitation. For example, the distance between carbon atoms in organic molecules is of the order of 0.1 nm, much shorter than the $2p \rightarrow 1s$ transition wavelength of ~ 4 nm. If a large enough number of carbon atoms is core-excited in a single FEL pulse, it is conceivable that superfluorescent decay may occur, competing with or even overwhelming Auger decay. It is

thus worth considering whether multiatom effects must be considered in the analysis of current experiments, and further, whether it may even be possible to exploit such effects in future experiments.

We are grateful to the RIKEN SCSS test accelerator engineering team for experimental support and stable operation of the accelerator.

*nagasono@spring8.or.jp

- [1] T. Shintake, H. Tanaka, T. Hara, T. Tanaka, K. Togawa, M. Yabashi, Y. Otake, Y. Asano, T. Bizen, and T. Fukui *et al.*, *Nat. Photon.* **2**, 555 (2008).
- [2] W. Ackermann, G. Asova, V. Ayvazyan, A. Azima, N. Baboi, J. Bähr, V. Balandin, B. Beutner, A. Brandt, and A. Bolzmann *et al.*, *Nat. Photon.* **1**, 336 (2007).
- [3] E. Allaria, C. Callegari, D. Cocco, W.M. Fawley, M. Kiskinova, C. Masciovecchio, and F. Parmigiani, *New J. Phys.* **12**, 075002 (2010).
- [4] P. Emma, R. Akre, J. Arthur, R. Bionta, C. Bostedt, J. Bozek, A. Brachmann, P. Bucksbaum, R. Coffee, and F. Decker *et al.*, *Nat. Photon.* **4**, 641 (2010).
- [5] G. Geloni, E. Saldin, L. Samoylova, E. Schneidmiller, H. Sinn, T. Tschentscher, and M. Yurkov, *New J. Phys.* **12**, 035021 (2010).
- [6] R.A. Bartels, A. Paul, H. Green, H.C. Kapteyn, M.M. Murnane, S. Backus, I.P. Christov, Y. Liu, D. Attwood, and C. Jacobsen, *Science* **297**, 376 (2002).
- [7] F. Krausz and M. Ivanov, *Rev. Mod. Phys.* **81**, 163 (2009).
- [8] Y. Wang, E. Granados, F. Pedaci, D. Alessi, B. Luther, M. Berrill, and J.J. Rocca, *Nat. Photon.* **2**, 94 (2008).
- [9] S. Suckewer and P. Jaegl, *Laser Phys. Lett.* **6**, 411 (2009).
- [10] H.C. Kapteyn and R.W. Falcone, *Phys. Rev. A* **37**, 2033 (1988).
- [11] K. Lan, E.E. Fill, and J. Meyer-ter-Vehn, *Europhys. Lett.* **64**, 454 (2003).
- [12] J. Zhao, Q.L. Dong, S.J. Wang, L. Zhang, and J. Zhang, *Opt. Express* **16**, 3546 (2008).
- [13] N. Rohringer and R. London, *Phys. Rev. A* **80**, 013809 (2009).
- [14] M.S. Feld and J.C. MacGillivray, in *Coherent Nonlinear Optics*, Topics in Current Physics Vol. 21 (Springer, Berlin, 1980), p. 7.
- [15] R.H. Dicke, *Phys. Rev.* **93**, 99 (1954).
- [16] N.E. Rehler and J.H. Eberly, *Phys. Rev. A* **3**, 1735 (1971).
- [17] E. Paradis, B. Barrett, A. Kumarakrishnan, R. Zhang, and G. Raithel, *Phys. Rev. A* **77**, 043419 (2008).
- [18] G.O. Ariunbold, M.M. Kash, V.A. Sautenkov, H. Li, Y.V. Rostovtsev, G.R. Welch, and M.O. Scully, *Phys. Rev. A* **82**, 043421 (2010).
- [19] M.O. Scully and A.A. Svidzinsky, *Science* **325**, 1510 (2009).
- [20] P. Hammond, *J. Electron Spectrosc. Relat. Phenom.* **144–147**, 13 (2005).
- [21] A. Kumarakrishnan and X.L. Han, *Phys. Rev. A* **58**, 4153 (1998).
- [22] H. Ohashi, Y. Senba, M. Nagasono, M. Yabashi, K. Tono, T. Togashi, T. Kudo, H. Kishimoto, T. Miura, H. Kimura,

- and T. Ishikawa, *Nucl. Instrum. Methods Phys. Res., Sect. A* **649**, 163 (2011).
- [23] W. F. Chan, G. Cooper, and C. E. Brion, *Phys. Rev. A* **44**, 186 (1991).
- [24] G. W. F. Drake and D. C. Morton, *Astrophys. J. Suppl. Ser.* **170**, 251 (2007).
- [25] Q. H. F. Vreken and M. F. H. Schuurmans, *Phys. Rev. Lett.* **42**, 224 (1979).
- [26] M. Nagasono, E. Suljoti, A. Pietzsch, F. Hennies, M. Wellhfer, J. Hoefl, M. Martins, W. Wurth, R. Treusch, and J. Feldhaus *et al.*, *Phys. Rev. A* **75**, 051406 (2007).
- [27] H. W. van der Hart and P. Bingham, *J. Phys. B* **38**, 207 (2005).
- [28] A. Hishikawa *et al.* (to be published).
- [29] D. Polder, M. F. H. Schuurmans, and Q. H. F. Vreken, *Phys. Rev. A* **19**, 1192 (1979).
- [30] T. Togashi, E. J. Takahashi, K. Midorikawa, M. Aoyama, K. Yamakawa, T. Sato, A. Iwasaki, S. Owada, T. Okino, and K. Yamanouchi *et al.*, *Opt. Express* **19**, 317 (2011).
- [31] H. N. Chapman, P. Fromme, A. Barty, T. A. White, R. A. Kirian, A. Aquila, M. S. Hunter, J. Schulz, D. P. DePonte, and U. Weierstall *et al.*, *Nature (London)* **470**, 73 (2011).
- [32] M. M. Seibert, T. Ekeberg, F. R. N. C. Maia, M. Svenda, J. Andreasson, O. Jonsson, D. Odic, B. Iwan, A. Rocker, and D. Westphal *et al.*, *Nature (London)* **470**, 78 (2011).